

Magnetic and transport properties of $\text{Pb}_{1-x}\text{Mn}_x\text{Te}$ spin-glass

M. Escorne and A. Mauger

*Physics Department, University of California, Irvine, California 92717
and Laboratoire de Physique des Solides, Centre National de la Recherche Scientifique,
1 place A. Briand, F-92190 Meudon, France*

J. L. Tholence

*Centre de Recherche des Très Basses Températures, Centre National de la Recherche Scientifique,
Boîte Postale 166X, F-38042 Grenoble, France*

R. Triboulet

*Laboratoire de Physique des Solides, Centre National de la Recherche Scientifique,
1 place A. Briand, F-92190 Meudon, France*

(Received 9 September 1983)

Magnetic properties of $\text{Pb}_{1-x}\text{Mn}_x\text{Te}$ are reported for Mn concentrations $x \leq 0.2$. Below 1 K, a spin-glass behavior is observed, characterized by a thermoremanent magnetization which has been studied as a function of time and of the magnetic field. The freezing temperature T_g defined by a cusp in the reversible part of the magnetic susceptibility is found to be associated with the occurrence of a spin-glass state rather than a clustering effect as in the other manganese compound $\text{Cd}_{1-x}\text{Mn}_x\text{Te}$. We attribute this result to the existence of long-range interband exchange interactions arising from the fact that $\text{Pb}_{1-x}\text{Mn}_x\text{Te}$ is a small-gap semiconductor. For all Mn concentrations, antiferromagnetic interactions are shown to dominate, in opposition with previous theoretical predictions. Above T_g , the material is in a superparamagnetic state due to short-range antiferromagnetic superexchange interactions. It is shown that a mean-field approximation accounts very well for the experimental results, above a temperature $T_M \sim 2T_g$ up to a magnetic field $H \sim 10$ kG, but breaks down at $T < T_M$. This effect is related to the pathological behavior of the functional dependence of the magnetization on the magnetic field above the de Almeida–Thouless instability temperature. All the samples were *p* type. The transport experiments show that the valence band is significantly perturbed upon introduction of Mn in the matrix. In particular, a crossing between valleys of the valence band with extrema at the *L* points of the Brillouin zone and the valleys with extrema along the Σ (symmetry) directions, is inferred at $x \sim 0.114$ at low temperatures. At high magnetic field, the magnetoresistance associated with the diffusion of holes by the spin fluctuations is shown to be positive, although a negative magnetoresistance can be observed in the low-field limit on some samples.

I. INTRODUCTION

A considerable amount of work has been done on the study of the class of materials known as semimagnetic semiconductors. Indeed, the subject has been introduced by M. Rodot and co-workers who investigated the exchange interactions of manganese ions (Mn^{2+}) diluted in II-VI compounds in the late 1960s.¹⁻³ The host matrix is either SnTe ,¹ GeTe ,² or PbTe .³ Mn^{2+} is the most convenient impurity, because of its electronic configuration $3d^5$ with zero orbital momentum (*s* state). Then, there is no spin-orbit interaction giving rise to anisotropy effects, and the experimental results are interpreted more easily. The magnetic properties of $\text{Ge}_{1-x}\text{Mn}_x\text{Te}$ and $\text{Sn}_{1-x}\text{Mn}_x\text{Te}$ are well understood: The ferromagnetic ordering of these alloys is due to the Ruderman-Kittel-Kasuya-Yosida (RKKY) interaction mediated by the 10^{20} – 10^{21} cm^{-3} free carriers (holes).⁴ The carrier concentrations in $\text{Pb}_{1-x}\text{Mn}_x\text{Te}$, however, are much smaller, and so is the RKKY interaction, so that the magnetic behavior of this material is much more complex. Magnetic suscep-

tibility measurements have already been published independently by Andrianov *et al.*,⁵ and Hamasaki.⁶ In the temperature range $77 < T < 300$ K, Hamasaki found that a Curie-Weiss law was satisfied, with values of the paramagnetic Curie temperature Θ very small, and even $\theta \sim 0$ within experimental uncertainty. This result is very different from those of Andrianov *et al.*,⁵ who found that the Curie-Weiss law was not satisfied in the lower part of this temperature range, at least for lowest manganese concentrations (≤ 0.016). Moreover, they reported huge values of Θ . The most striking disagreement appears for $x = 0.016$ (x or concentration, is in units of at. % throughout), because samples with such a Mn concentration have been studied by both groups (actually $x = 0.015$ in Ref. 6). In that case the reported values of Θ are 70 (Ref. 5) and 0 K.⁶ However, measurements at lower temperatures showed that there is no magnetic freezing in the whole range investigated, $4.2 < T < 300$ K,⁵ and thus there is at least one point on which all authors agree, namely that the magnetic interactions in $\text{Pb}_{1-x}\text{Mn}_x\text{Te}$ are small. One purpose of this paper is to study the magnetic proper-

ties of $\text{Pb}_{1-x}\text{Mn}_x\text{Te}$ at low temperatures ($T \leq 100$ K), especially in the range $0.09 < T < 4.2$ K which has not yet been investigated. It is shown, in particular, that $\text{Pb}_{1-x}\text{Mn}_x\text{Te}$ undergoes a spin-glass transition below 1 K. We also infer the existence of Mn clusters. The proportion of Mn ions frozen in such antiferromagnetic clusters is, however, not much larger than the value expected from statistical fluctuations in the average composition, in the framework of a random distribution of the Mn ions in the host matrix, except at the highest Mn concentrations. The different results in Refs. 5 and 6 are analyzed and imputed to such magnetic clustering effects, as well as some other specific properties in our own samples.

Usually, transport properties of magnetic semiconductors are not as spectacular as the magnetic properties. Ford and Mydosh⁷ found that the impurity resistivity in spin-glasses varies roughly linearly with temperature around the freezing temperature T_g , and then shows a broad maximum at a temperature T_m much larger than T_g . However, the application of an external magnetic field is expected to significantly modify the spin correlations. Consequently, the localized spins contribute significantly to the magnetic resistance. The second purpose of this paper is to investigate some transport properties of $\text{Pb}_{1-x}\text{Mn}_x\text{Te}$, namely Hall effect and resistivity as a function of the temperature and the magnetic field. In particular, we show that the variations of these quantities as a function of temperature are dominated by modifications in the band structure of PbTe, induced by the introduction of Mn ions in the matrix. We also show that the Mn ions not frozen in the clusters give rise to a *positive* contribution to the magnetoresistance at least at high magnetic field. This feature shows that $\text{Pb}_{1-x}\text{Mn}_x\text{Te}$ is not a canonical spin-glass. This result is associated with the fact that the ferromagnetic coupling induced by the external magnetic field competes with the antiferromagnetic superexchange interactions which are shown to dominate at all the Mn concentrations investigated.

Since the clustering effects are important, there is an ambiguity in the definition of x . The nominal composition x_n is equal to the value of x averaged over a volume which is larger compared to the lattice parameter (and then to the size of the magnetic clusters). The effective concentration x_{eff} is the concentration of manganese ions which are not inside the clusters. The range of compositions investigated are $x_n \leq 0.20$ and $x_{\text{eff}} \leq 0.06$.

The distinction between x_n and x_{eff} is the cornerstone of the analysis of our experimental data. It also emphasizes the necessity of specifying the procedure used to prepare the sample, since the concentration of clusters and their size may vary widely depending on the metallurgical procedure used. This is the object of the second section. In Sec. III the magnetic susceptibility measurements are reported. The discussion of the results is reported in Sec. IV.

II. SAMPLE PREPARATION

Crystal growth has been carried out by the Bridgman method under tellurium vapor pressure in a three-zone

furnace as described in Ref. 8 for the growth of $\text{Cd}_{1-x}\text{Mn}_x\text{Te}$ alloys. Ingots with initial compositions ranging from 0.03 up to 0.5 have been grown by weighing appropriate amounts of PbTe, Mn, and Te, or Pb, Mn, and Te (6N Pb and Te, 3N 5 Mn). The growth rate used was 2.8 mm/h. The ingots were generally constituted by very large single crystals.

Three methods have been used for the "metallurgical" characterization of the samples: scanning electron microscopy (SEM), electron-microprobe measurements, and x-ray diffraction experiments. Only a single phase is visible in crystals with $x_n \leq 0.1$, from SEM observations, even at high magnification ($8000\times$). However, a fine eutectic-like structure is visible at high magnification in slices cut in ingots with $x_n = 0.15$ and 0.2, since MnTe-richer phases are found from Mn images. For $x_n \sim 0.5$ extra phases are clearly visible even at low magnification: Important MnTe zones are found in an eutecticlike Pb-rich background.

It is worth noticing that a good radial homogeneity and reproducible values are found from electron-microprobe measurements in samples with $x_n = 0.15$ and 0.20. This discrepancy with the SEM observation is likely to be due to the diffusion volume of the electron beam, which is very important as is its impact area. The variations of Mn composition, as determined by electron-microprobe analysis, is reported as a function of the distance d from the bottom of the ingots along the axis in Figs. 1 and 2. The normal freezing in the case of partial mixing in non-volatile liquids is expressed by the law⁹

$$x_n(d) = kc_0(1-d/l)^{k-1}. \quad (2.1)$$

Here, x_n is the concentration of manganese in the ingot, k is the interface distribution coefficient, c_0 is the initial value of the uniform concentration of solute in the liquid,⁹ and l is the total length of the ingot.

For $x_n \cong 0.03$ and $x_n \sim 0.1$, the experimental data can

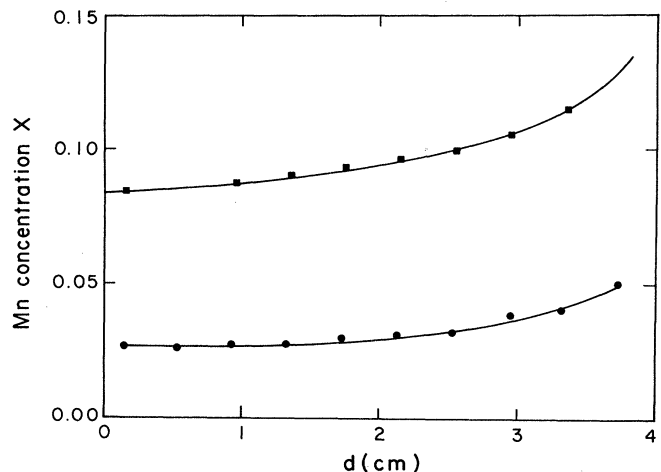


FIG. 1. Manganese concentration x in $\text{Pb}_{1-x}\text{Mn}_x\text{Te}$ as a function of the distance d from the extremity of the ingot for two low Mn concentrations. Solid circles and squares are experimental data. The solid curves are theoretical and are derived from the Pfann law [see Eq. (2.1)].

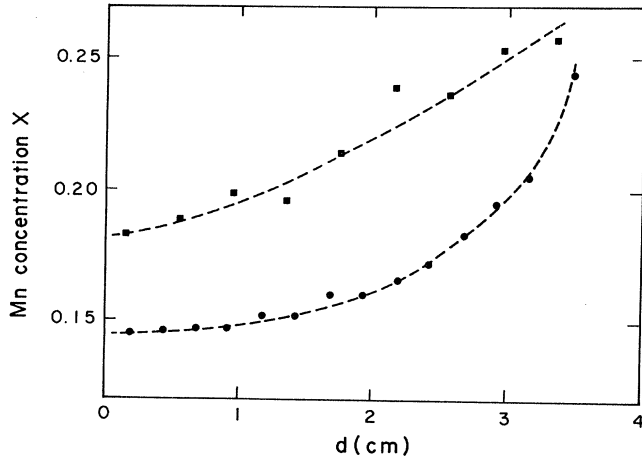


FIG. 2. Manganese concentration x in $\text{Pb}_{1-x}\text{Mn}_x\text{Te}$ as a function of the distance d from the extremity of the ingot for two larger Mn concentrations. The dashed curves are guides for the eyes, and the data could not be fitted theoretically, due to the heterogeneity of the material.

actually be fitted by Eq. (2.1) (see Fig. 1). This confirms the solid-solution character of alloys of composition ranging up to $x_n \sim 0.1$. To the contrary, the experimental points of Fig. 2 cannot be fitted by the expression (2.1). This still confirms that alloys with $x_n = 0.15$ and 0.2 are heterogeneous.

As mentioned above, the alloys have also been studied by x-ray diffraction. Lead telluride has a cubic NaCl structure with a lattice parameter, measured in our samples, equal to 6.46 \AA , in agreement with previous results.¹⁰ Alloys up to $x_n = 0.1$ keep the same structure, and their parameters seem to follow Vegard's law, as shown in Fig. 3. On the contrary, crystals with $x_n \sim 0.15$ present additional lines corresponding to hexagonal MnTe. The lines associated with PbTe are split in triplets, indicating a deformation of the cubic NaCl structure towards an hexagonal structure. The extra MnTe lines are not visible in the spectra of crystals with $x_n = 0.2$, but the very weak intensity and resolution of these spectra reveal a very poor crystallographic quality. The lattice parameters determined for the cubic PbTe-rich phase present in the $x_n = 0.15$ and 0.20 samples are not reproducible, and correspond to alloys of lower Mn concentrations. For $x_n = 0.15$ and 0.20 the alloys are then constituted by a microscopic, finely divided eutecticlike structure with a very fine MnTe phase in a PbTe-rich background. However, homogeneous $\text{Pb}_{1-x}\text{Mn}_x\text{Te}$ has been prepared up to $x_n = 0.115$. This result is in agreement with that of Vanuyarkho,¹¹ who reported that the solubility limit of MnTe in PbTe is $x = 0.12$. Indeed, the highest composition of manganese in $\text{Pb}_{1-x}\text{Mn}_x\text{Te}$ alloys for which physical properties have been reported is $x = 0.12$.¹² Up to now, however, only the Soviet "school" has published data with Mn compositions larger than 4 at. %. The homogeneous samples ($x_n \leq 0.12$) can be characterized by the chemical formula $\text{Pb}_{1-x}\text{Mn}_x\text{Te}$ with $x = x_n$, without any ambiguity. For the $x_n = 0.20$ sample, however, such notation is no longer justified. For convenience, we shall still refer to this sample as the " $x = 0.20$ sample," keeping in mind

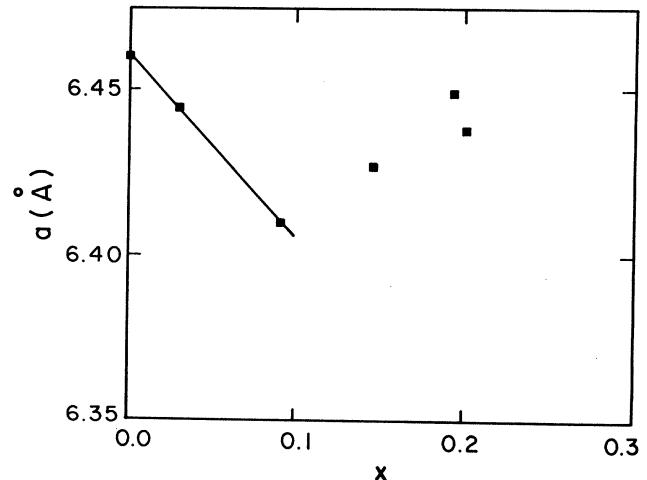


FIG. 3. Variations of the lattice parameter a as a function of the Mn concentration x in $\text{Pb}_{1-x}\text{Mn}_x\text{Te}$. The solid curve outlines the low-concentration range where a linear law is observed.

that this notation does not have any chemical signification in this particular case.

III. MAGNETIC MEASUREMENTS

All the samples presented a deviation from the Curie law at low temperatures (below 1 K). This will now be shown to correspond to a micromagnetic or a spin-glass transition.

A. Characterization of the spin-glass state

The most prominent feature associated with the existence of frozen spins without long-range order is the shift of the magnetization curve relative to the applied-field origin, yielding remanent magnetization for field-cooled samples. Since this remanent magnetization is usually small, the spin-glass properties of the systems are studied for low cooling fields so that irreversible effects may be compared to the reversible ones. The results are reported in Figs. 4–6. The cooling field is $H = 160 \text{ G}$ ex-

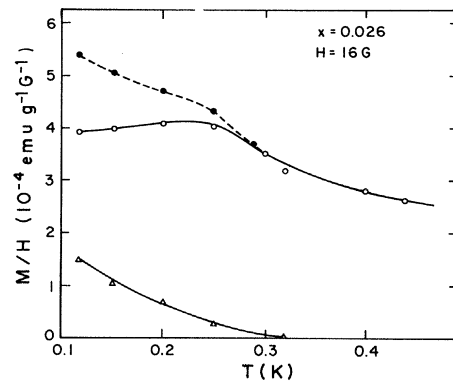


FIG. 4. Magnetic susceptibility of $\text{Pb}_{1-x}\text{Mn}_x\text{Te}$ for $x = 0.026$, measured in a field of 16 G . Experimental points are represented by solid circles for the total magnetic susceptibility, open circles for the reversible part of the susceptibility, and triangles, for the irreversible part proportional to the TRM.

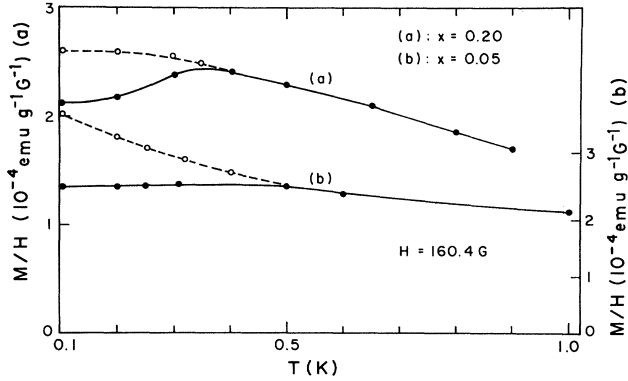


FIG. 5. Magnetic susceptibilities of $\text{Pb}_{1-x}\text{Mn}_x\text{Te}$ for $x=0.20$ [curve (a), left scale] and 0.05 [curve (b), right scale], in a field $H=160.4$ G. Experimental points are represented by open circles for the total magnetic susceptibility and solid circles for the reversible part of the susceptibility.

cept for $x_n=0.026$ where $H=16$ G, because in this latter case the irreversible effects were even smaller. For higher cooling fields, the maximum of susceptibility can still be observed, but is more rounded. This is a common feature of spin-glasses.¹³ The freezing temperature T_g defined by the susceptibility cusp is reported in Table I for the various samples investigated. Since the magnetic properties of the sample depend on their history below T_g , it is important to specify the procedure used in the experiments.

The samples have been cooled from over T_g to $T < T_g$ in a field H . The corresponding magnetization is the so-called total magnetization $M_{\text{tot}}(T, H)$. We have checked that the chosen magnetic field H is always small enough so that $M_{\text{tot}}(T, H) \propto H$. It follows that we can define the total magnetic susceptibility by

$$\chi_{\text{tot}}(T) = M_{\text{tot}}(T, H) / H. \quad (3.1)$$

If at a constant temperature $T < T_g$ the applied field H is suddenly removed, we are left with the thermo-remanent magnetization $\mathcal{M}_{\text{tr}}(T, H, t)$ (outside of

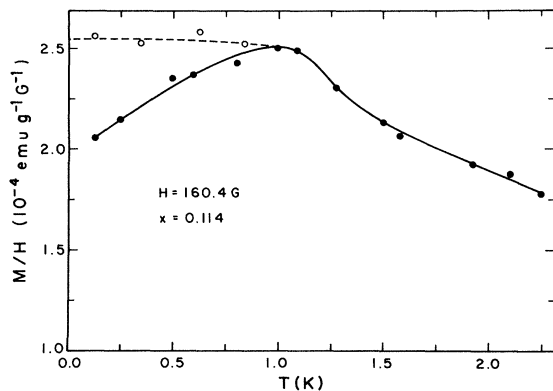


FIG. 6. Magnetic susceptibility of $\text{Pb}_{1-x}\text{Mn}_x\text{Te}$ for $x=0.114$ in a field $H=160.4$ G. Experimental points are represented by open circles for the total susceptibility and by solid circles for reversible susceptibility.

mathematical constructions, we will use the acronym TRM) and since we are in the low-field limit, we can define the reversible susceptibility as

$$\chi_{\text{rev}}(T, t) = \frac{M_{\text{tot}}(T, H) - \mathcal{M}_{\text{tr}}(T, H, t)}{H}. \quad (3.2)$$

Here t is the time after the withdrawal of the external field H . Then the field is applied before any change of temperature. In most spin-glasses, the relaxation time τ above which the remanant magnetization has dropped is long, perhaps say hours or even days, so that the time dependence of $\chi_{\text{rev}}(T, t)$ can be neglected at the time scale of the experiments ($t \sim 0$). Such is not the case for $\text{Pb}_{1-x}\text{Mn}_x\text{Te}$ mainly because the lowest temperature available is still important compared to T_g . This is illustrated in Fig. 7 where we have reported $\mathcal{M}_{\text{tr}}(T=0.1 \text{ K}, H, t)$ as a function of $\ln t$, for $H=10$ G and 160.4 G, in the case $x_n=0.026$. It then appears that $\tau \approx 1$ min in our sample. For technical reasons, it was not possible to reach the limit $t \sim 0$, and all the curves $\chi_{\text{rev}}(T, t)$ plotted in Figs. 2 and 4 are for $t=20$ s.

There is no cusp in the total susceptibility curve $\chi_{\text{tot}}(T, H)$. This is a common feature of spin-glasses.¹⁴ The $x=0.026$ case, however, is singular, because $\chi_{\text{tot}}(T, H)$ is not saturated at low temperatures ($T < T_g$). Such a behavior is usually observed in materials such as $\text{Eu}_{1-x}\text{Sr}_x\text{S}$ at low magnetic impurity concentrations,¹⁵ where the results are interpreted in terms of magnetic clustering rather than spin-glass behavior.¹⁰ However, in such a case the reversible part of the magnetic susceptibility should also increase as T is decreased below T_g , due to the contribution of the "loose" spins to χ_{rev} , which satisfies a Curie-Weiss law. This has been clearly observed in $\text{Cd}_{1-x}\text{Mn}_x\text{Te}$ (Ref. 16) and in spinels.¹⁷ Conversely, in $\text{Pb}_{1-x}\text{Mn}_x\text{Te}$ the reversible susceptibility decreases monotonically upon cooling below the temperature of the cusp T_g , even for small Mn concentrations, $x \sim 0.026$. This is the standard behavior of magnetic spin-glasses, and

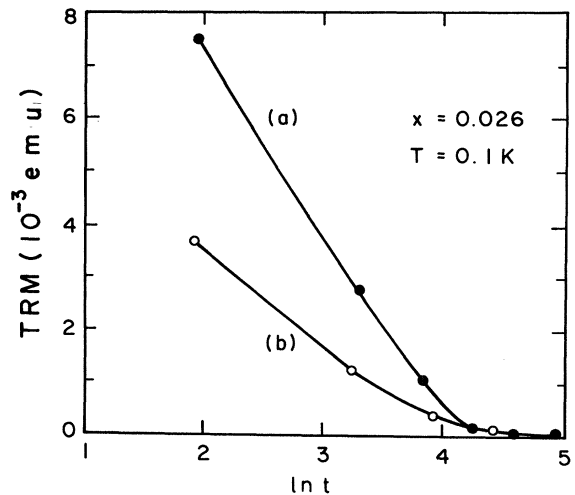


FIG. 7. TRM as a function of neperian logarithm of time in $\text{Pb}_{1-x}\text{Mn}_x\text{Te}$ for $x=0.026$, at a temperature $T=0.1$ K, after field cooling in 1043 [curve (a)] and 1604 G [curve (b)]. The time is expressed in s.

indeed, in this material T_g can be considered as the temperature of transition towards a spin-glass state. This difference is due to the fact that in $\text{Pb}_{1-x}\text{Mn}_x\text{Te}$, the indirect exchange interactions are supposed to be long ranged, so that they can drive a collective freezing of the magnetic spin at low temperatures, contrary to the case of $\text{Cd}_{1-x}\text{Mn}_x\text{Te}$, where the interactions are short ranged. This will be discussed in more detail hereafter.

For completeness of our characterization of the spin-glass state, we have explored the magnetic field dependence of \mathcal{M}_{tr} ($T=0.1, M, t=20$ s) for various samples (Fig. 8). The TRM goes through a maximum and then decreases. At still higher magnetic fields, the TRM is expected to saturate at a value $\mathcal{M}_r(T, t)$, where \mathcal{M}_r is the remanent magnetization (RM outside of mathematical constructions) independent of M . In practice, however, it was difficult to determine \mathcal{M}_r , either because the RM value was reached at too high a magnetic field (large x), or because \mathcal{M}_r was too small (small x). Then, the TRM (shown in Fig. 9 for $x=0.15$) is very small at low temperature, and a rapid drop of the TRM is observed just below T_g (0.6 K for $x=0.15$). This is in contrast with the classical behavior of $\mathcal{M}_{\text{tr}}(T)$ in spin-glass which is linear for small cooling fields¹⁸ or exponential-like when the TRM is saturated.¹⁹

B. Magnetic properties above T_g

Above T_g the thermoremanent magnetization vanishes. There is no longer any irreversible effect, and the low-field magnetic susceptibility is defined by

$$\chi(T) = \lim_{M \rightarrow 0} \frac{M(T, H)}{H} \quad (3.3)$$

We found that $\chi(T)$ defined above obeys a Curie-Weiss law,

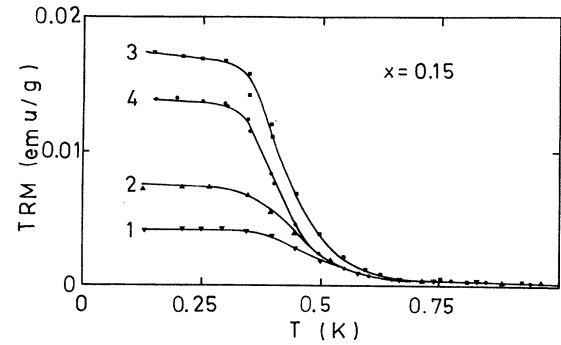


FIG. 9. TRM as a function of temperature in $\text{Pb}_{0.85}\text{Mn}_{0.15}\text{Te}$ at various magnetic fields $H=100$ (curve 1), 200 (curve 2), 1500 (curve 3), and 2500 G (curve 4).

$$\chi(T) = x_{\text{eff}} \frac{N_0 S(S+1)}{3k_B(T+\Theta)} g^2 \mu_B^2 \quad (3.4)$$

for all the samples investigated, up to 100 K. x_{eff} is the effective concentration x of loose manganese ions, not frozen in antiferromagnetic clusters, N_0 is the number of unit cells, g is the Lande factor, μ_B is the Bohr magneton, and k_B is the Boltzmann constant. x_{eff} has been deduced from Eq. (3.4), assuming that $S = \frac{5}{2}$ and $g=2$ for the Mn^{2+} ions. The Curie-Weiss law is illustrated in Fig. 10 for $x_n=0.114$ in the entire range $4.2 < T < 100$ K. The values of Θ and x_{eff} for the various samples are reported in Table I. Morris had already reported that a Curie-Weiss law was obeyed in this range of temperatures.²⁰ Moreover, we have found that the same law is obeyed down to the temperature $T_M \sim 2T_g$, as shown in Figs. 11 and 12 for $x < 0.11$. For $x=0.15$ and 0.20, a slight downwards curvature of $\chi^{-1}(T)$ is observed, giving a Curie-Weiss temperature depending on the temperature range

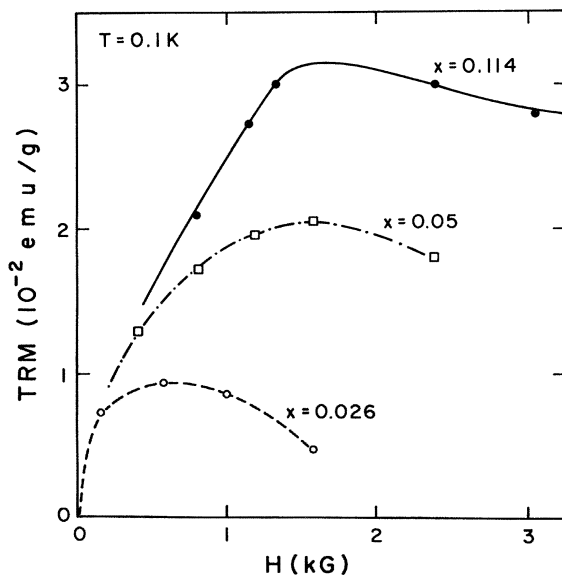


FIG. 8. TRM in $\text{Pb}_{1-x}\text{Mn}_x\text{Te}$ as a function of the magnetic field for various concentrations x , at temperature $T=0.1$ K, and time $t=20$ s.

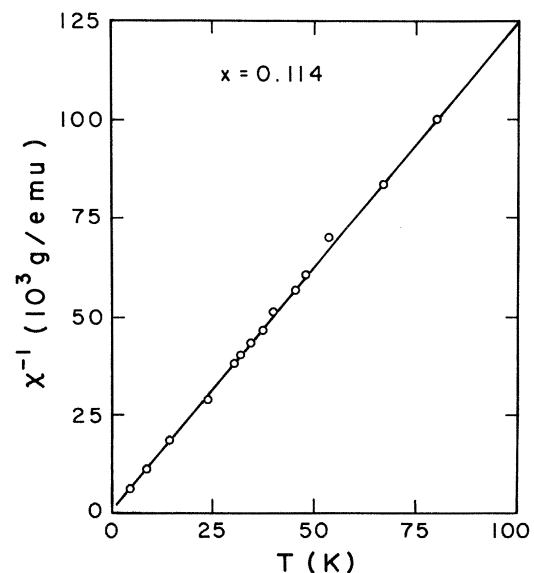


FIG. 10. Inverse of the magnetic susceptibility in the superparamagnetic range of temperatures for $\text{Pb}_{1-x}\text{Mn}_x\text{Te}$ with $x=0.114$.

TABLE I. Characteristic properties of the $\text{Pb}_{1-x}\text{Mn}_x\text{Te}$ samples studied in this paper. x_{eff} is the effective manganese concentration not frozen in spin clusters in the superparamagnetic phase, as deduced from magnetic data. x_{eff}^* is the theoretical value, taking into account the formation of antiferromagnetic pairs and assuming a random distribution of the Mn ions in the matrix. Θ is the paramagnetic Curie temperature. The footnotes denote, for the heterogeneous samples, the temperature ranges (used to fit the magnetic susceptibility curve by the Curie law) on which Θ depends.

Samples	x_{eff} (at. %)	x_{eff}^* (at. %)	Θ (K)	T_g (K)	ρ (cm^{-3})	μ ($\text{cm}^2 \text{V}^{-1} \text{s}^{-1}$)
$\text{Pb}_{0.974}\text{Mn}_{0.026}\text{Te}$	1.52	1.89	-0.07	0.25		
$\text{Pb}_{0.95}\text{Mn}_{0.05}\text{Te}$	2.46	2.70	-3.0	0.50	2.2×10^{19}	450
$\text{Pb}_{0.886}\text{Mn}_{0.114}\text{Te}$	6.06	2.67	-1.8	1.0	6.5×10^{17}	4
$\text{Pb}_{0.853}\text{Mn}_{0.147}\text{Te}$	9.09	2.18	-2.6 ^a -5.0 ^b	0.6		
$\text{Pb}_{0.80}\text{Mn}_{0.20}\text{Te}$	2.72	1.37	-2.0 ^a -2.5 ^b	0.35	6.3×10^{16}	28

^a $1 < T < 4.2$ K.

^b $5 < T < 20$ K.

explored (see Table I). The fact that $x_n \neq x_{\text{eff}}$ means that above T_g , the system is in a superparamagnetic state characterized by isolated antiferromagnetic clusters of Mn ions embedded in a paramagnetic matrix. This result is in qualitative agreement with those reported for $\text{Cd}_{1-x}\text{Mn}_x\text{Te}$ alloys.^{16,21} Using a more quantitative point of view, however, we notice that the concentration $x_n - x_{\text{eff}}$ of Mn spins inside the clusters, which do not contribute to the magnetic properties (below 100 K), is not very different from the values we have previously reported for $\text{Cd}_{1-x}\text{Mn}_x\text{Te}$,¹⁶ except for $x_n = 0.20$. For comparison, we found $x_{\text{eff}} = 0.03, 0.04,$ and 0.056 for $x_n = 0.05, 0.10,$ and $0.20,$ respectively, in $\text{Cd}_{1-x}\text{Mn}_x\text{Te}$. Galazka *et al.*²¹ concluded that there is a large deviation of the repartition of Mn ions with respect to the statistical distribution in this material. The similarity of the results obtained in $\text{Pb}_{1-x}\text{Mn}_x\text{Te}$ and $\text{Cd}_{1-x}\text{Mn}_x\text{Te}$ makes this interpretation more questionable. In fact, quantitative calculations of x_{eff} can only be made in the limit of small Mn concentrations. In that case, only two configurations

of Mn ions have a significative probability to occur in a statistical distribution, namely single ions and pairs. Since the pairs are antiferromagnetically coupled by the strong superexchange interaction, the only Mn ions which contribute to the magnetic properties in the range of temperature investigated are single ions. In the fcc lattice each atom has 12 first neighbors, so that the value of x_{eff} in a statistical distribution is

$$x_{\text{eff}}^* = x_n(1 - x_n)^{12}. \quad (3.5)$$

The values of x_{eff}^* are also reported in Table I for comparison with the value deduced from experimental data. The agreement of x_{eff}^* and x_{eff} is very good for $x_n \leq 0.05$. At higher concentrations, where larger clusters enter into account, Eq. (3.4) underestimates the value of x_{eff} for obvious reasons: Owing to the frustration of the antiferromagnetic interactions specific to the topology of the fcc lattice,^{22,23} the internal exchange field may locally vanish for certain manganese ions which, however, have one or several Mn first neighbors. Such manganese ions also contribute to the magnetic susceptibility, as do the single ones. This process is not considered by Galazka *et al.*²¹ and is not taken into account in Eq. (3.5). On the other

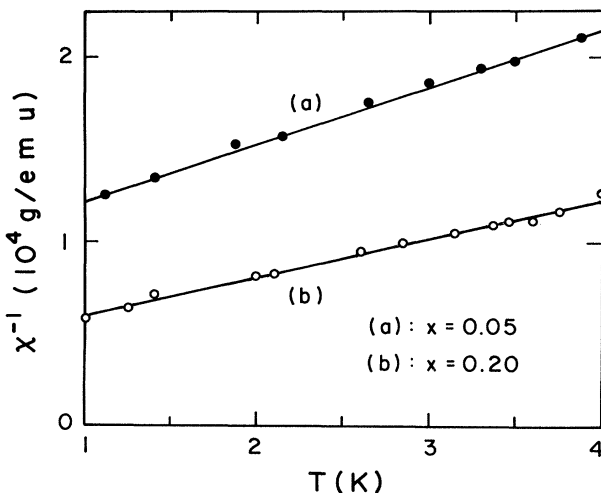


FIG. 11. Inverse of the magnetic susceptibility above T_g , as a function of temperature for $\text{Pb}_{1-x}\text{Mn}_x\text{Te}$ at concentrations $x = 0.05$ and 0.20 .

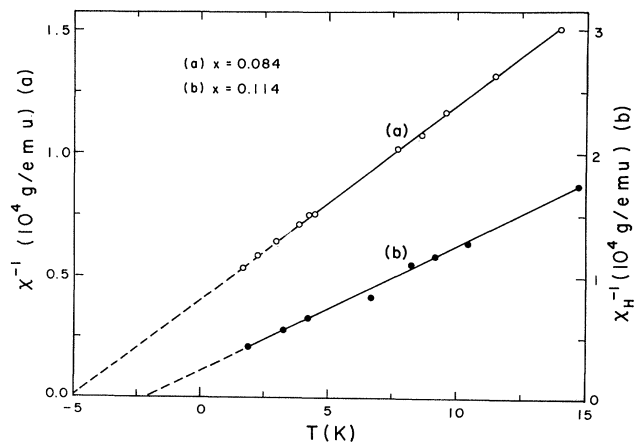


FIG. 12. Inverse of the magnetic susceptibility above T_g in $\text{Pb}_{1-x}\text{Mn}_x\text{Te}$ for $x = 0.084$ and 0.114 .

hand, Eq. (3.5) supposes that the range of the magnetic interactions is limited to first neighbors; a longer range is more realistic and implies a lower value of x_{eff} . Then, any detailed calculation becomes not only difficult, but also hazardous, because it requires some hypothesis on the strength and range of magnetic interactions between Mn ions. Qualitatively, however, the good agreements between x_{eff} observed in $\text{Pb}_{1-x}\text{Mn}_x\text{Te}$ and $\text{Cd}_{1-x}\text{Mn}_x\text{Te}$ for $x_n \sim 0.11$ indicates that at this concentration the deviation of the Mn distribution from the statistical one is insignificant. It is clear, however, that such a deviation exists in $\text{Pb}_{0.80}\text{Mn}_{0.20}\text{Te}$ where x_{eff} drops to 0.027. This result is clearly associated with the fact that the limit of dilution x_n of Mn in $\text{Pb}_{1-x}\text{Mn}_x\text{Te}$ is much smaller than in $\text{Cd}_{1-x}\text{Mn}_x\text{Te}$, and it points out the heterogeneity of $\text{Pb}_{0.80}\text{Mn}_{0.20}\text{Te}$, as evidenced in Sec. II.

In the range $100 < T < 300$ K, the susceptibility curve $\chi(T)$ is dominated by the contribution of manganese pairs in antiferromagnetic clusters, which are frozen at lower temperatures due to the direct superexchange interaction. This explains the very large values of the paramagnetic Curie temperatures reported in Ref. 5. It is clear, however, that the pertinent parameter Θ must be deduced from data at lower temperatures, since the frozen clusters do not provide any significant contribution to any physical property at $T < 100$ K, which is just the range of temperatures of interest where the physical properties of semimagnetic semiconductors distinguish this class of materials from canonical semiconductors.

Equation (3.4) is an indication that the molecular-field approximation can be used to describe the magnetic properties above T_g , or at least above T_M . To check this important hypothesis, we have measured the magnetization curves $M(H)$ above T_g for fields up to 10 kG using a Foner-type vibrating-sample magnetometer. The results for $x_n = 0.114$ are reported in Fig. 13. In a molecular-field theory, the magnetization is given by the Brillouin law,

$$M(x_{\text{eff}}, T, H) = x_{\text{eff}} N_0 S B_{5/2}(g\mu_B SH / k_B(T + \Theta)). \quad (3.6)$$

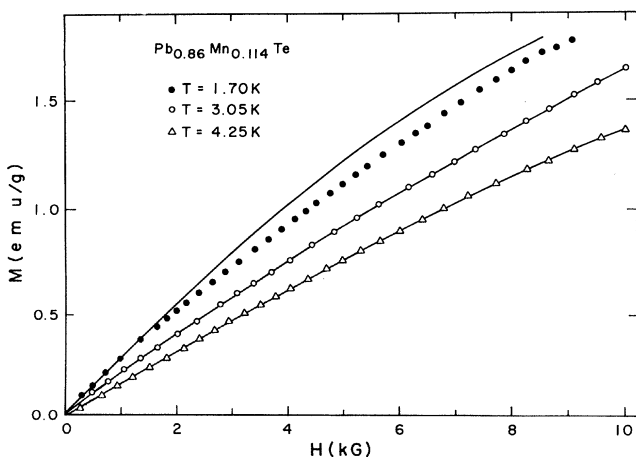


FIG. 13. Magnetization curve as a function of the magnetic field above the freezing temperature in $\text{Pb}_{0.86}\text{Mn}_{0.114}\text{Te}$. Circles and triangles represent experiment points. The solid curves are theoretical, according to the Brillouin law.

$B_{5/2}$ is the Brillouin function for the spin $S = \frac{5}{2}$. To be self-consistent, Θ and x_{eff} are chosen to be the same as the parameters derived from Eq. (3.4) and low-field susceptibility data. It follows that Eq. (3.6) does not contain any unknown parameter. A very good quantitative agreement between experiments and the theoretical law in Eq. (3.6) has been found for the whole range of magnetic fields explored, $0 \leq H \leq 10$ kG, down to the temperature $T_M \sim 2T_g$. A similar agreement has also been observed for $\text{Cd}_{1-x}\text{Mn}_x\text{Te}$.^{16,24} At smaller temperatures, we still find that Eq. (3.4) is satisfied in the low magnetic field limit, as can be seen in Fig. 13; at higher fields, however, very significant deviations of the experimental curve from the Brillouin law in Eq. (3.6) are observed, with a magnetization lower than the predicted value. This result establishes the limit of validity of the molecular-field approximation which breaks down below a temperature $T_M(H) > T_g$, with $T_M \sim 2T_g$ at $H \sim 10$ kG.

Sherrington and Kirpatrick (SK) have developed a mean-field theory for spin-glasses, in absence of magnetic field (SK model).²⁵ The SK solution is indeed stable in the paramagnetic phase ($T > T_g$), but not in the spin-glass state where a negative entropy is found. This is consistent with the fact that $T_M(H \rightarrow 0) = T_g(H = 0) = T_g$ and the fact that Eq. (3.4) was satisfied down to the lowest temperatures investigated above T_g in our samples. However, in the presence of a magnetic field H , the SK solution is stable at temperatures $T > T_g(H)$, where $T_g(H) < T_g$ is the de Almeida–Thouless instability line.²⁶ Our results show that there is a range of temperatures $T_g(H) < T < T_M(H)$ where the molecular-field approximation is not valid, with the magnetization $M(H)$ departing from the value predicted by the Brillouin law. $T_M(H)$ can be considered as the reciprocal function of the law $H_m(T)$ representing the crossover line Curie–non-Curie paramagnet which has been evidenced in Cu:Mn.²⁷ Although more general expressions can be derived,²⁸ the development of the magnetization in terms of odd powers of H is generally used,

$$M = A_1(T)H - A_3(T)M^3 + A_5(T)H^5 + \dots$$

$A_1(T) = \chi(T)$ is the first-order magnetic susceptibility given by Eq. (3.4), but the higher-order susceptibilities A_3, A_5, \dots diverge at T_g . This behavior has been confirmed experimentally by several authors in the spin-glass $(\text{Ti}_x\text{V}_{1-x})_2\text{O}_3$ (Ref. 29) and in the metallic spin-glass Cu-Mn.³⁰ Following the authors of Ref. 30, we have plotted $M/(\chi H)$ vs H^2 in Fig. 14. The initial slope of this curve is the coefficient A_3 , which is found to increase by a factor of 15 between 3.05 and 1.70 K for the $x = 0.114$ sample. We have investigated the A_3 coefficient in detail in the close vicinity of T_g and in low fields ($H < 500$ G).³¹ Contrary to what has been observed in Cu-Mn, this coefficient does not diverge with $[T/(T - T_g)]^\gamma$. If the divergence of A_3 is taken as a criterion for a “transition” in spin-glasses, there is no transition in $\text{Pb}_{1-x}\text{Mn}_x\text{Te}$.

IV. DISCUSSION

The spin-glass temperature T_g does not depend significantly on the carrier concentration. This is clearly evidenced by comparison of the data in Table I. In particu-

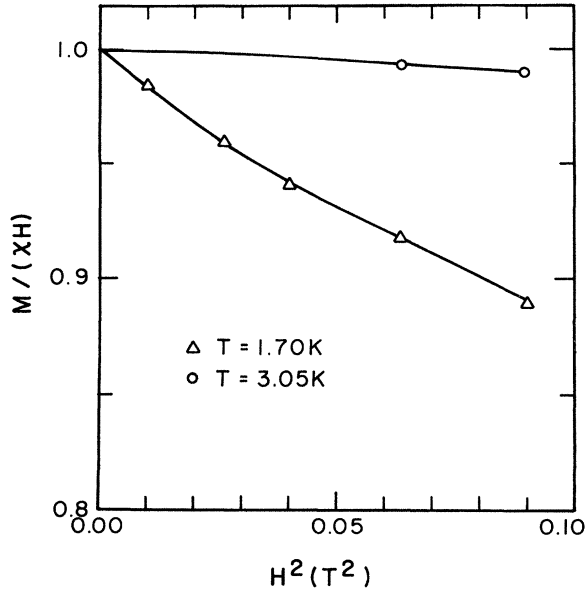


FIG. 14. Variations of $M/\chi H$ vs H^2 in $\text{Pb}_{0.86}\text{Mn}_{0.14}\text{Te}$ at two temperatures: 3.05 and 1.70 K. M is the magnetization in the field H and χ is the low-field magnetic susceptibility. The slope of the curves is the coefficient of H^3 in the series development of the magnetization vs H .

lar, the two samples which have similar values of x_{eff} , namely $x_{\text{eff}} = 2.46 \times 10^{-2}$, have also similar values of T_g although the carrier concentrations differ by 3 orders of magnitude. It follows that the intraband indirect exchange mediated by the free carriers (RKKY interaction) does not contribute significantly to the freezing process. A further evidence of this conclusion is provided by the analysis of the paramagnetic Curie temperature Θ which is always negative, even for the highest carrier concentration $p = 2 \times 10^{19} \text{ cm}^{-3}$. For such carrier concentrations ($p < 10^{20} \text{ cm}^{-3}$), however, the jellium approximation does apply and the RKKY interaction is essentially ferromagnetic,⁴ leading to a positive contribution to Θ . Two reasons may explain why the RKKY interaction is negligible in $\text{Pb}_{1-x}\text{Mn}_x\text{Te}$. First the mobility of the free carriers is much smaller than in $\text{Sn}_{1-x}\text{Mn}_x\text{Te}$ or $\text{Ge}_{1-x}\text{Mn}_x\text{Te}$ where the RKKY interaction is strong enough to drive a ferromagnetic ordering. The RKKY coupling constant then reads³²

$$J(R_{ij}) = \frac{9\pi}{4} \frac{p^2}{E_F} J_{sd}^2 F(2k_F R_{ij}) e^{-R_{ij}/\lambda}, \quad (4.1)$$

where $F(y) = (\sin y - y \cos y)/y^4$ is the range function, λ is the mean free path of the holes, k_F is the Fermi wave vector, and E_F is the Fermi energy. The exponential factor is actually a strong damping in $\text{Pb}_{1-x}\text{Mn}_x\text{Te}$. Second, nuclear-magnetic-resonance experiments have revealed that the exchange integral J_{sd} between the free carriers and the localized Mn spins is very small.³³ Since J_{sd} enters to the square in the expression of $J(R_{ij})$, a small value of J_{sd} strongly contributes to make the RKKY exchange inefficient.

We can also notice that the same samples with

$x_{\text{eff}} = 9.46 \times 10^{-2}$ and $x_{\text{eff}} = 2.72 \times 10^{-2}$ have quite different values of x_n , and then a quite different number of Mn spins frozen in antiferromagnetic cluster, although they have almost the same value of T_g . We can then infer that the Mn ions frozen in clusters do not participate to the spin-glass freezing. This is confirmed by the quasilinear variation of T_g as a function of x_{eff} , evidenced in Fig. 15. We can understand this effect as follows. Antiferromagnetic clusters of Mn ions are formed under the effect of the superexchange interaction. Such interactions are short range in nature and cannot drive a collective freezing of the magnetic spins unless the concentration x of Mn ions is larger than the critical percolation threshold x_c , namely 0.136 in the fcc lattice, for interactions extending up the next-nearest neighbors.³⁴ Indeed, we have shown¹⁶ that the spin freezing of $\text{Cd}_{1-x}\text{Mn}_x\text{Te}$ could be interpreted in the framework of a spin-cluster blocking theory, since the range of the magnetic interaction is smaller than the mean distance between Mn ions. In particular, no cusp of the magnetic susceptibility has been reported in $\text{Cd}_{1-x}\text{Mn}_x\text{Te}$ for $x \leq 0.15$. Oseroff *et al.*³⁵ have observed such a peak only at $x \geq 0.15$, this critical concentration being very close to x_c .

The existence of a spin-glass freezing at lower Mn concentrations in $\text{Pb}_{1-x}\text{Mn}_x\text{Te}$ suggests the onset of a long-range indirect interaction. For a semiconductor with parabolic conduction and valence bands characterized by effective masses m_e and m_h , respectively, Abrikosov has shown that the interband exchange is of the form³⁶

$$J_{\text{eff}}(R_{ij}) = \pi^{-5/2} \left[\frac{\alpha m_e m_h}{m_e + m_h} \right]^{3/2} \times [2(m_e + m_h)]^{-1/2} \frac{e^{-\alpha R_{ij}}}{R_{ij}^{5/2}} \psi(\vec{R}_{ij}). \quad (4.2)$$

$\psi(R_{ij})$ is an oscillating factor. For nonparabolic bands, such as in Pb-Te, the range function is more complex and

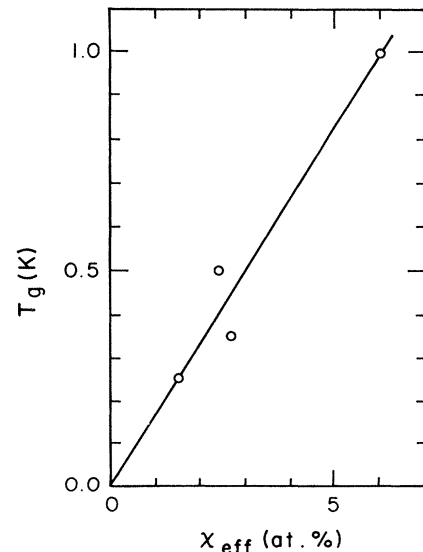


FIG. 15. Variations of the spin-glass temperature T_g as a function of the effective concentration x_{eff} of Mn spins not frozen in the superparamagnetic configuration.

is replaced by a Bessel function,³⁷ which, however, changes the results only quantitatively. The important feature is that in semiconductors with a large gap E_g , the damping coefficient

$$\alpha = [2E_g(m_e + m_h)]^{1/2} \quad (4.3)$$

is large, and the interaction decreases exponentially with the distance. This is the specific property of the Bloembergen-Rowland interaction,³⁸ and the experimental situation met in $\text{Cd}_{1-x}\text{Mn}_x\text{Te}$. In small-gap semiconductors such as $\text{Pb}_{1-x}\text{Mn}_x\text{Te}$, however, α is small and the interband indirect exchange becomes long ranged. Let us now investigate the properties of the function ψ . If one of the bands has its extremum at the center of the Brillouin zone and the other one has valleys at wave vectors \vec{K}_l , we have³⁶

$$\psi(R_{ij}) = \sum_l \cos(\vec{K}_l \cdot \vec{R}_{ij}), \quad (4.4)$$

the generalization to $\text{Pb}_{1-x}\text{Mn}_x\text{Te}$ where both the conduction and valence bands have extrema at the L points is trivial and reads

$$\psi(R_{ij}) = \sum_{l,m} \cos[(\vec{K}_l - \vec{K}_m) \cdot \vec{R}_{ij}], \quad (4.5)$$

where \vec{K}_l and \vec{K}_m are wave vectors belonging to the set $\langle 111 \rangle$. It follows that $\vec{K}_l - \vec{K}_m$ is a reciprocal-lattice vector and all the cosines entering $\psi(R_{ij})$ are equal to unity. So we are left with the puzzling result that in this very particular case, the interaction does not oscillate and is always ferromagnetic.³⁷ Nevertheless, the spin-glass freezing which is associated with the concept of frustration implies the existence of oscillations in the long-range exchange interaction. Such oscillations in $\psi(\vec{R}_{ij})$ are restored by the existence of a finite carrier concentration, since the virtual electron-hole transitions are possible for electron states at an energy E_F and not at the extremum of the band. Then, $\psi(R_{ij})$ oscillates with a period of oscillations k_F^{-1} such as RKKY interactions. However, for the low carrier concentrations available, k_F^{-1} is very large so the interband exchange still remains essentially ferromagnetic, as the RKKY exchange interaction.

We are thus led to the conclusion that the two-band model which neglects spin-orbit interaction is not sufficient to properly calculate the indirect exchange interaction. In fact, six bands are separated only by spin-orbit interactions at the L points,³⁹ and not only two. This gives rise to new interband interactions which on the average could be negative. A similar situation is met in europium chalcogenides where interactions between p , f , and d bands compete,⁴⁰ except that in that case the interactions are short ranged because the energy gaps are large.

The violation of the Brillouin law at $T = 1.7$ K can be considered as a pretransitional effect, the spin-correlation function being strongly affected by the application of a magnetic field at a temperature close to T_g . Further evidence of this interpretation will be provided by the analysis of transport properties in the same range of temperatures and magnetic fields.

V. TRANSPORT PROPERTIES

Transport properties are known to be very sensitive to the band structure. That of PbTe is rather complex, but has been extensively studied and is well known. Weak field magnetoresistance,⁴¹⁻⁴³ piezoresistance,^{44,45} measurements of de Haas-Van Alphen,⁴⁶ and Shubnikov-de Haas^{47,48} effects, as well as Azbel-Kaner cyclotron^{49,51} effects, have shown that the extrema of the principal valence band are located at the L points of the Brillouin zone, and that the constant energy surfaces for the four valleys issuing from the L points are prolate in the $[111]$ direction. Evidence for the population of lower-energy valence-band valleys has been found in the temperature^{52,53} and pressure⁵⁴ dependence of the Hall coefficient and in the temperature dependence of the electric susceptibility mass.⁵⁵ Band-structure calculations⁵⁶ have accounted for the existence of secondary maxima of the valence band located along the Σ axis. Let us denote ΔE_v as the energy gap between these two types of valence-band extrema. A simplified picture of the band structure is reported in Fig. 16. Optical-absorption data⁵⁷ suggest that $\Delta E_v \sim 0.08$ eV at 300 K, while analysis of the temperature dependence of the Hall coefficient^{52,53} results in a gap of about 0.15 eV at 0 K, and thus

$$\frac{d\Delta E_v}{dT} \sim -2 \times 10^{-4}, \quad (5.1)$$

in eV/K. For comparison, the energy gap between the top of the valence band and the bottom of the conduction band is $E_g = 0.32$ eV (Ref. 58) at room temperature, and decreases upon cooling at a rate⁵⁵

$$\frac{dE_g}{dT} = 4.9 \times 10^{-4}, \quad (5.2)$$

in eV/K. These data allow us to adjust the relative position of the bands for PbTe, as illustrated in Fig. 16.

$\text{Pb}_{1-x}\text{Mn}_x\text{Te}$ alloys have been much less investigated. The only study of transport properties reported to our knowledge after the pioneer work of Toth *et al.*³ is the accurate work of Vinogradova *et al.*,¹² but only high temperatures were explored ($100 < T < 800$ K). The data were explained by an increase of E_g and a decrease of ΔE_v as

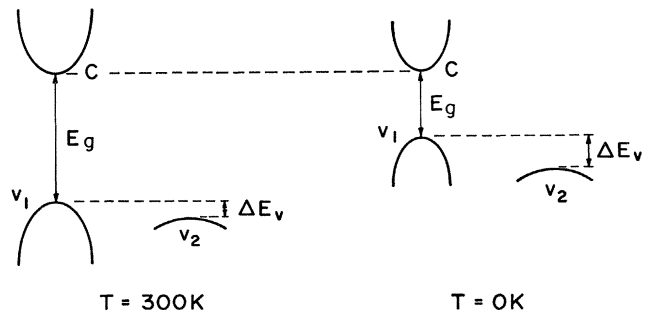


FIG. 16. Relative positions of the conduction and valence bands in PbTe as a function of temperature. The extrema of the conduction band and of the valleys v_1 are at the L point. v_2 is a second set of valleys along the Σ axis, belonging to the same valence band as v_1 .

x_n is increased. This result is in agreement with optical measurements⁵⁹ which provided a more quantitative expression of the variations of E_g with x_n (in units of eV),

$$\frac{dE_g}{dx} \simeq 1.3. \quad (5.3)$$

It is our purpose in this section to investigate the transport properties of $\text{Pb}_{1-x}\text{Mn}_x\text{Te}$, and to not only investigate the influence of manganese on the energy spectrum of holes in PbTe, but to also study the scattering of holes by the Mn ions. Although we will report measurements up to $T=300$ K, attention will be focused on low-temperature results ($1.5 \leq T \leq 4.2$ K). The first advantage when dealing with low temperatures is that transport properties are not smoothed by the spreading out of the Fermi energy. Second, electron-phonon scattering is small and, as we shall see, the holes are scattered by the thermal Mn spin fluctuations.

All the samples were p type. The transport properties of the $x_n=0.05$ and 0.20 samples were found to be very similar, which is due to the fact that x_{eff} is about the same in both samples (see Sec. III). The resistivity curves for $x_n=0.114$ and 0.20 are reported in Fig. 17. At high temperatures, the resistivity goes through a maximum, at $T \sim 160$ K for the $x_n=0.114$ sample and $T \sim 60$ K for the $x_n=0.20$ sample. This feature is not associated with the existence of Mn ions because it was also present in the resistivity curve of the PbTe matrix. Moreover, such a feature was not observed by other authors,⁵⁹ so that this bump of resistivity may be just an extrinsic property, and is probably associated with some resonant impurity introduced with Pb or Te. Two sharp anomalies at $T=20$ K for $x_n=0.114$ and $T \sim 90$ K for $x_n \sim 0.20$ were also observed, but were not explained. In the range $4.2 < T < 15$ K, the resistivity is practically independent of temperature, and the hole concentration p deduced from the Hall coefficient was also constant. This is illustrated in Fig. 18 where we have plotted the variations of the Hall resistivity as a function of the magnetic field for the $x=0.20$ sample. Strictly speaking, p is the "apparent" hole concentration, because an anisotropy factor r enters the expression

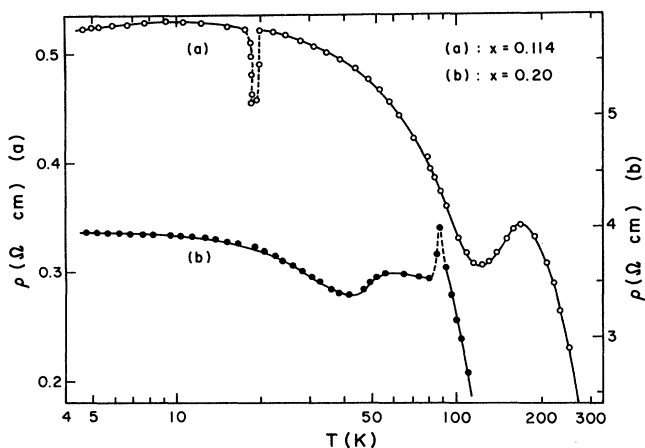


FIG. 17. Resistivity curves of $\text{Pb}_{1-x}\text{Mn}_x\text{Te}$ for $x=0.114$ [curve (a), left scale] and 0.20 [curve (b), right scale].

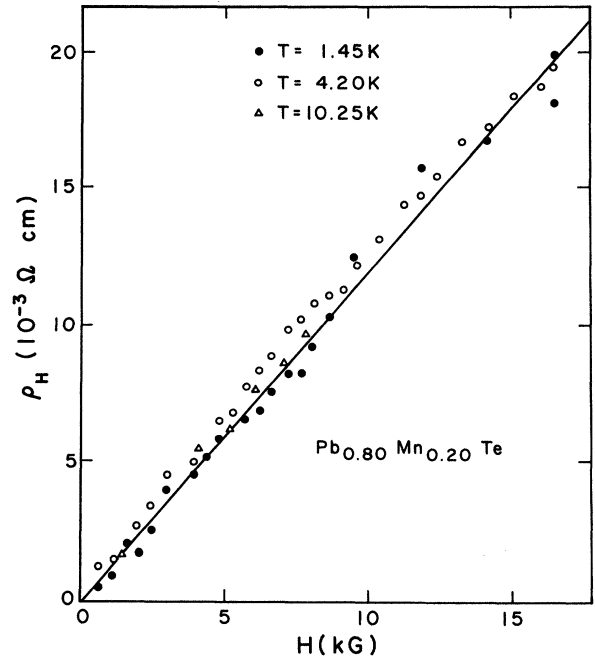


FIG. 18. Hall resistivity as a function of the magnetic field for $\text{Pb}_{0.80}\text{Mn}_{0.20}\text{Te}$, at various temperatures. The slope of the curve is the Hall coefficient.

of the Hall coefficient as a function of p ,³⁷ as in SnTe. However, this factor is close to unity for all carrier concentrations, and we shall neglect it for practical purposes. The hole concentration p and the Hall mobility μ at 4.2 K are reported in Table I.

Measurements were also performed in the range $1.5 < T < 4.2$ K. Except for the $x_n=0.114$ sample, the resistivity was a constant in this range of temperatures as it was in the range $4.2 < T < 15$ K. For the $x_n=0.114$ sample, however, a very large decrease of the resistivity, by a factor 10^4 is observed, as can be seen in Fig. 19. The Hall resistivity is reported as a function of H in Fig. 20 at $T=4.2$ and 2.18 K. At the lower temperature, this quantity was difficult to measure, and the dispersion of the experimental points is large, especially at low magnetic fields. We have analyzed elsewhere⁶⁰ the reasons for such a dispersion of the data when the resistivity depends strongly on temperature, which we observed in other magnetic semiconductors. The high-field data, however, are accurate enough to provide a determination of the Hall coefficient, and then a value of p . As can be seen in Fig. 20, the variation of p between 4.2 and 2.18 K, if any, is at most a factor of 2. This means that the drop of resistivity by a factor of 10^4 is due to a variation of the mobility and not to a variation in the number of carriers. Also, this large increase in the mobility of the holes upon cooling is not due to the onset of some superconducting state. The reason is that the application of magnetic fields available in the experiments, namely $H < 50$ kG, did not remove this effect: We shall see hereafter that there is only a factor-of-3 difference between the magnetoresistance at $T=1.45$ and 4.2 K at $H \sim 50$ kG. Such a high magnetic field should have canceled any superconducting effect. Also a superconductor is characterized by a strong di-

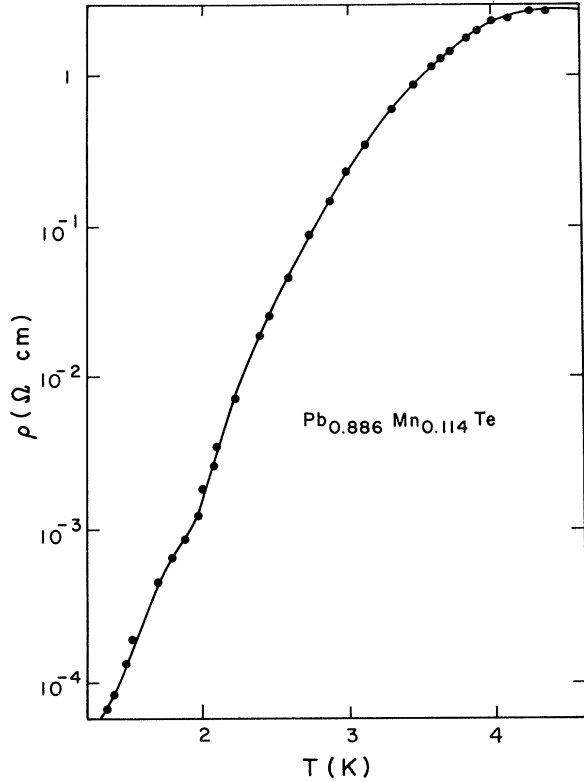


FIG. 19. Resistivity curve of $\text{Pb}_{0.886}\text{Mn}_{0.114}\text{Te}$ at low temperature. Solid circles represent experimental points.

amagnetic susceptibility. We have seen in Sec. III that the sample is paramagnetic, even if the magnetization is lower than that predicted by the Brillouin law.

We are thus led to the hypothesis that the large change in the hole mobility between 1.45 and 4.2 K for $x_n=0.114$ is due to a change in the valence-band structure, namely a crossing between the light-hole valleys v_1 issuing from the L points and the heavy-hole valence valleys v_2 issuing from the Σ axis. This interpretation is consistent with predictions on the valence-band structure. When taking

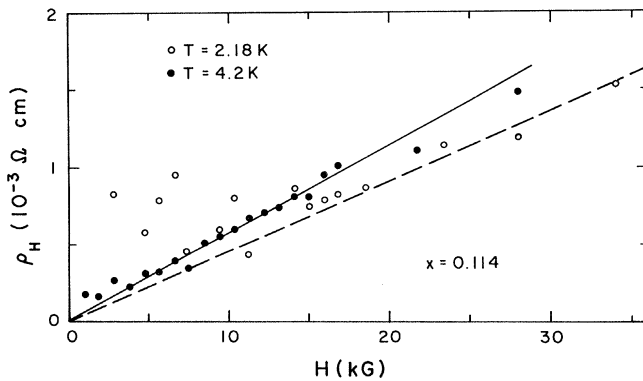


FIG. 20. Hall resistivity as a function of the magnetic field for $\text{Pb}_{0.886}\text{Mn}_{0.114}\text{Te}$ at low temperatures. Circles represent experimental points. The solid curve is the linear curve deduced from a least-squares fit of the data at $T=4.2$ K. The dashed curve is deduced from the mean-square fit of the data at $T=2.18$ K at magnetic fields $H > 10$ kG.

into account the relative values of E_g and ΔE_v in PbTe reported above, the comparison between Eqs. (4.1) and (4.2) shows that ΔE_v is expected to vanish for $E_g \simeq 450$ meV, and then, according to Eq. (4.3), such an energy gap is expected for $x=0.11$ at low temperatures (a value of $E_g \simeq 0.46$ eV has been reported in Ref. 59 at 10 K for $x=0.10$). The scheme of the valence band for the $x=0.114$ sample is then illustrated in Fig. 21: At $T < 4.2$ K, the holes occupy the light-hole valleys v_1 . Then at $T \sim 4.2$ K, there is a crossing between the two valence-band extrema, under the effect of the temperature coefficient, which, for such Mn concentrations, is⁵⁹ $dE_g/dT \sim 1.7 \times 10^{-4}$ eV/K, and the free carriers are then heavy holes in the v_2 valleys. To avoid some of the ambiguity encountered in the literature, it is worth noticing that v_1 and v_2 are *different* valleys belonging to the *same* valence band.⁵³ In particular, the crossing between v_1 and v_2 cannot be considered a valence-band crossing.

The magnetoresistance at 1.45 and 4.2 K is reported for $x_n=0.114$ in Fig. 22, and for $x_n=0.20$ in Fig. 23. The magnetoresistance measured in the experiments is the sum of two separate contributions,

$$(\Delta\rho/\rho)_{\text{meas}} = (\Delta\rho/\rho)_{\text{nor}} + (\Delta\rho/\rho)_{\text{mag}}.$$

$(\Delta\rho/\rho)_{\text{nor}}$ is the normal positive magnetoresistance of the matrix, which has been studied in detail for PbTe.⁴¹⁻⁴³ $(\Delta\rho/\rho)_{\text{mag}}$ is the contribution coming from Mn spin fluctuations. For $x_n=0.114$, $(\Delta\rho/\rho)_{\text{nor}}$ is negligible and we can write, within a good approximation,

$$(\Delta\rho/\rho)_{\text{meas}} = (\Delta\rho/\rho)_{\text{mag}}.$$

According to Fig. 22, $(\Delta\rho/\rho)_{\text{mag}}$ is essentially positive and goes through a maximum at $H \sim 25$ kG. This can be understood as follows. As one approaches T_g from above, the spin correlation at short distances increases due to the antiferromagnetic coupling between Mn ions. The application of a magnetic field first opposes this antiferromagnetic arrangement, which increases the spin fluctuations and the diffusion of the free carriers. So the resistivity first increases. Then, a further increase in H leads to the onset of partial ferromagnetic arrangement, which diminishes the spin fluctuations and then the resistivity. The field $H \sim 25$ kG for which $\Delta\rho/\rho$ is maximum then appears as the order of magnitude of the field which "breaks" the antiferromagnetic coupling of the $N_{0x_{\text{eff}}}$ Mn ions responsible for the spin-glass behavior at lower temperatures.

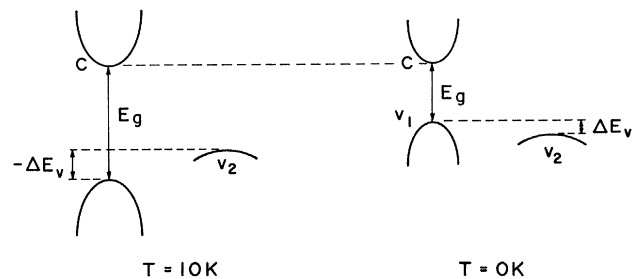


FIG. 21. Tentative diagram representing the band scheme of $\text{Pb}_{0.886}\text{Mn}_{0.114}\text{Te}$ at low temperature. Notations are the same as in Fig. 16.

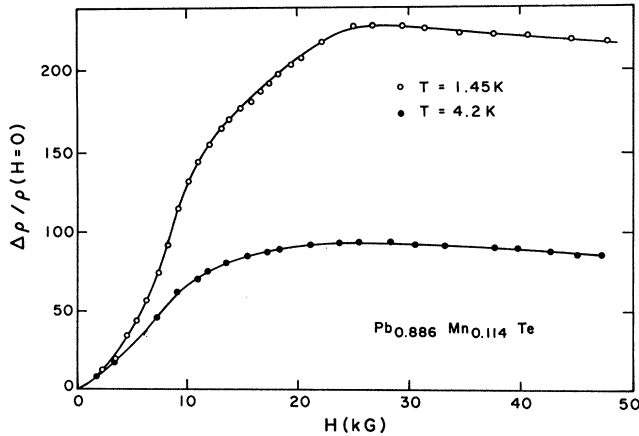


FIG. 22. Magnetoresistance $[\rho(H) - \rho(0)]/\rho(0)$ as a function of the magnetic field for $x=0.114$ at two low temperatures.

For $x_n \simeq 0.20$ or 0.05 , x_{eff} is very small (~ 0.025), so that now, $(\Delta\rho/\rho)_{\text{nor}}$ and $(\Delta\rho/\rho)_{\text{mag}}$ have the same order of magnitude (the Mn spins frozen in clusters, in concentration $x_n - x_{\text{eff}}$, do not contribute to the magnetoresistance at such temperatures). We can see in Fig. 23 that a bump in the magnetoresistance curve is superimposed on the positive background $(\Delta\rho/\rho)_{\text{nor}}$ outlined by the dashed curve. *A priori*, this bump looks like a Shubnikov-de Haas oscillation. However, the very low mobility of the free carriers makes observation of any oscillation of that kind even at $H \sim 50$ kG impossible, and the nature of this bump must be very different: It can be considered the $(\Delta\rho/\rho)_{\text{mag}}$ part of the magnetoresistance similar to that reported in Fig. 22, but with a reduced magnitude, superimposed on $(\Delta\rho/\rho)_{\text{nor}}$. $(\Delta\rho/\rho)_{\text{mag}}$ has quite the same field dependence as the $x=0.114$ sample, except that the magnetic field H at which $(\Delta\rho/\rho)_{\text{mag}}$ is maximum is slightly shifted at lower magnetic field ($H \sim 15$ kG), which is consistent with the fact that the antiferromagnetic interactions and the freezing temperature T_g are smaller than in the $x=0.114$ sample. The temperature dependence of $(\Delta\rho/\rho)_{\text{mag}}$ is also the same as for the $x=0.114$ sample, namely $(\Delta\rho/\rho)_{\text{mag}}$ increases as T decreases because then the temperature becomes closer to T_g and spin fluctuations are enhanced. At low magnetic fields, it can be seen in Fig. 23 that $(\Delta\rho/\rho)_{\text{meas}}$ is negative, which is a canonical behavior of spin-glasses⁶¹ on both sides of T_g .

VI. CONCLUSION

Below 100 K we have established that the molecular-field approximation gives a good description of the magnetic properties down to very low temperatures ($T_N \sim 2T_g$). We found that the paramagnetic Curie temperature Θ is very small for all the concentrations. This result is in agreement with previous data, not only of Ref. 6, but also of Ref. 5 if we restrict ourselves to low temperatures ($T < 100$ K). Moreover, Θ was negative at all Mn concentrations. This is in opposition to theoretical results predicted by the Abrikosov model³⁶ of the indirect-exchange mechanism in such semiconductors. This model predicts that the indirect-exchange interaction in the limit of vanishing carrier concentrations is ferromagnetic. Liu

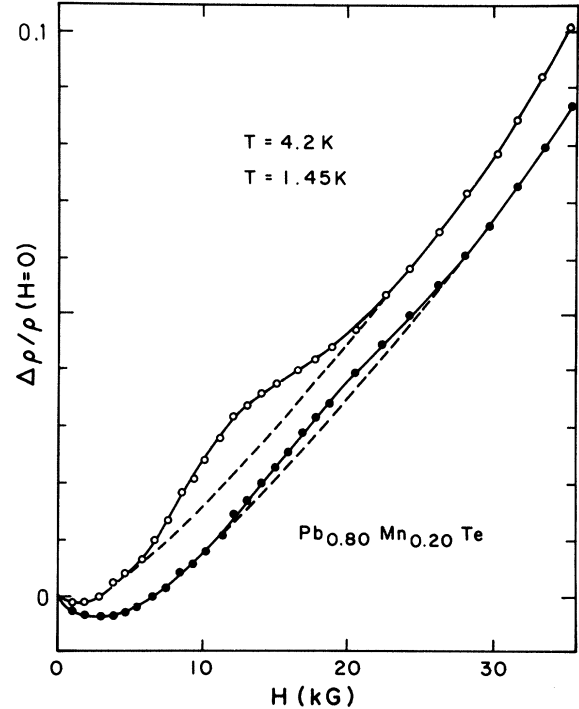


FIG. 23. Magnetoresistance $[\rho(H) - \rho(0)]/\rho(0)$ for $x=0.20$ at temperatures $T=4.2$ and 1.45 K.

and Bastard³⁷ emphasized that a crossing between valleys v_1 and v_2 would even increase this ferromagnetic interaction, since new channels are then opening up for electron-hole excitations. This conclusion of Ref. 37, however, may not be true. The reason is that the function $\psi(R_{ij})$ in Eq. (4.2) associated with the contribution of the extrema of the valence band along the Σ axis at wave vectors $\vec{\kappa}_m$ reads

$$\psi(R_{ij}) = \sum_{e,m} \cos[(\vec{\kappa}_l - \vec{\kappa}_m) \cdot \vec{R}_{ij}].$$

This is a form similar to Eq. (4.5), with $\vec{\kappa}_l$ the wave vectors of the set $\langle 111 \rangle$ corresponding to the valleys of the conduction band at the L point. The difference is that $\vec{\kappa}_l - \vec{\kappa}_m$ is no longer a reciprocal-lattice vector, so that $\psi(R_{ij})$ is now an oscillating function. It follows that the existence of an extremum of the valence band along the Σ axis gives rise to a long-range interband interaction oscillating as a function of the distance. Such an interaction does not increase ferromagnetic interactions, but generates frustrations in the magnetic interactions which are required for the spin-glass behavior. This may explain why magnetic properties did not show any particular anomaly in the $x=0.114$ sample, where we have reported some evidence of a crossing between v_1 and v_2 . Further experiments are required to confirm the crossing of these valleys which is already consistent with an anomalous behavior of the thermoelectric power observed for $x=0.1$.¹²

The deformation of the valence band is also responsible for the considerable drop of the hole mobility associated with the presence of manganese in $\text{Pb}_{1-x}\text{Mn}_x\text{Te}$, since the energy gap increases with x , as does the mass of density of states at the Fermi level.

- ¹J. Cohen, A. Globa, P. Mollard, M. Rodot, and M. Rodot, *J. Phys. (Paris)* **29**, 142 (1968).
- ²J. E. Lewis and M. Rodot, *J. Phys. (Paris)* **29**, 352 (1968).
- ³G. Toth, J. Y. LePoup, and M. Rodot, *Phys. Rev. B* **1**, 4573 (1970).
- ⁴See for example, A. Mauger, thèse de doctorat d'état, Paris, 1980, and references therein.
- ⁵D. G. Andrianov, S. A. Belokon, V. M. Lakeenkov, A. S. Savel'ev, V. I. Fistul', and G. P. Tsiskarishvili, *Fiz. Tekh. Poluprovodn.* **12**, 2224 (1978) [*Sov. Phys.—Semicond.* **12**, 1323 (1979)].
- ⁶T. Hamasaki, *Solid State Commun.* **32**, 1069 (1979).
- ⁷J. A. Mydosh, P. J. Ford, M. P. Kawatra, and T. E. Whall, *Phys. Rev. B* **10**, 2845 (1974); P. J. Ford and J. A. Mydosh, *ibid.* **14**, 2057 (1976); *J. Phys. (Paris) Colloq.* **35**, C4-241 (1974).
- ⁸R. Triboulet and G. Didier, *J. Cryst. Growth* **52**, 614 (1981).
- ⁹S. E. Bradshaw and A. J. Mlavski, *J. Electron.* **2**, 134 (1956); J. C. Brice, in *Selected Topics in Solid State Physics*, edited by E. P. Wohlfarth (Wiley-Interscience, New York, 1965), Chap. 3, pp. 73–78.
- ¹⁰W. B. Pearson, in *Handbook of Lattice Spacings and Structure of Metals* (Pergamon, Oxford, 1967), Vol. 2.
- ¹¹V. G. Vanyarkho, Author's Abstract of Dissertation for Candidate's Degree (in Russian), Moscow State University, 1969.
- ¹²M. N. Vinogradova, N. V. Kolomoets, and L. M. Sysoeva, *Fiz. Tekh. Poluprovodn.* **5**, 218 (1971) [*Sov. Phys.—Semicond.* **5**, 186 (1971)].
- ¹³V. Cannella and J. Mydosh, *Phys. Rev. B* **6**, 4220 (1976).
- ¹⁴J. L. Tholence, thèse de Doctorat d'état, Grenoble, 1973.
- ¹⁵J. L. Tholence, F. Holtzberg, M. Godfrin, M. V. Lohreysen, and R. Tournier, *J. Phys. (Paris) Colloq.* **39**, C6-928 (1978); *J. Tholence, J. Appl. Phys.* **50**, 7369 (1979).
- ¹⁶M. Escorne and A. Mauger, *Phys. Rev. B* **25**, 4674 (1982).
- ¹⁷D. Fiorani, S. Viticoli, J. L. Dormann, M. Nogues, J. L. Tholence, J. Hamman, and A. P. Murani, *J. Magn. Magn. Mater.* **31-34**, 1393 (1983).
- ¹⁸H. Bouchiat and P. Monod, *J. Magn. Magn. Mater.* **30**, 175 (1982), and references therein.
- ¹⁹J. L. Tholence and R. Tournier, *Physica* **86-88&BC**, 873 (1977).
- ²⁰A. Morris, M.S. thesis, McGill University, Montreal, 1980.
- ²¹R. R. Galazka, S. Nagata, and P. M. Keesom, *Phys. Rev. B* **22**, 3344 (1980).
- ²²L. De Seze, *J. Phys.* **10**, L353 (1977).
- ²³A. Aharony, *J. Phys. C* **11**, L457 (1978).
- ²⁴J. A. Gaj, R. Planel, and G. Fishman, *Solid State Commun.* **29**, 435 (1979).
- ²⁵D. Sherrington and S. Kirpatrick, *Phys. Rev. Lett.* **35**, 1972 (1975).
- ²⁶J. R. L. De Almeida and D. J. Thouless, *J. Phys. A* **11**, 983 (1978).
- ²⁷A. Berton, J. Chaussy, J. Odin, R. Rammal, and T. Tournier, *J. Phys. Lett.* **43**, L153 (1982).
- ²⁸M. Susuki, *Prog. Theor. Phys.* **58**, 1151 (1977); *J. Chalupa, Solid State Commun.* **22**, 315 (1977).
- ²⁹S. Chikazawa, C. J. Sandberg, and Y. Miyako, *J. Phys. Soc. Jpn.* **50**, 2884 (1981).
- ³⁰R. Omari, J. J. Prejean, and J. Souletie, *J. Phys. (Paris)* **44**, 1069 (1983).
- ³¹J. L. Tholence, A. Benoît, M. Escorne, A. Mauger, and R. Triboulet, *Solid State Commun.* **49**, 417 (1984).
- ³²P. J. de Gennes, *J. Phys. Radium* **23**, 630 (1962).
- ³³B. Perrin and F. T. Hedgcock, *J. Phys. C* **15**, 6037 (1982).
- ³⁴C. Domb and N. W. Dalton, *Proc. Phys. Soc. London* **89**, 859 (1966).
- ³⁵S. B. Oseroff, R. Calvo, and W. Giriat, *Solid State Commun.* **35**, 539 (1980).
- ³⁶A. A. Abrikosov, *Adv. Phys.* **29**, 869 (1980).
- ³⁷L. Liu and G. Bastard, *Phys. Rev. B* **25**, 487 (1982).
- ³⁸N. Bloembergen and T. J. Rowland, *Phys. Rev.* **97**, 1679 (1955).
- ³⁹J. O. Dimmock and G. B. Wright, *Phys. Rev.* **135**, A821 (1964).
- ⁴⁰T. Kasuya, *IBM J. Res. Dev.* **14**, 214 (1970).
- ⁴¹K. Shogenji and S. Uchiyama, *J. Phys. Soc. Jpn.* **12**, 1164 (1957).
- ⁴²R. S. Allgaier, *Phys. Rev.* **119**, 554 (1960).
- ⁴³R. S. Allgaier, in *Proceedings of the International Conference on the Physics of Semiconductors, Prague, 1960* (Czechoslovak Academy of Sciences, Prague, 1961), p. 1037.
- ⁴⁴L. E. Hollander and T. J. Diesel, *J. Appl. Phys.* **31**, 622 (1960).
- ⁴⁵J. R. Burke, B. B. Houston, and R. S. Allgaier, *Bull. Am. Phys. Soc.* **6**, 136 (1961).
- ⁴⁶P. J. Stiles, E. Burstein, and D. N. Langenberg, *J. Appl. Phys.* **32**, 2174 (1961).
- ⁴⁷K. F. Cuff, M. R. Ellett, and C. D. Kuglin, in *Report of the International Conference on the Physics of Semiconductors, Exeter, 1962* (Institute of Physics, London, 1962), p. 316.
- ⁴⁸K. F. Cuff, M. R. Ellett, C. D. Kuglin, and L. R. Williams, in *Proceedings of the International Conference on the Physics of Semiconductors, Paris, 1964*, edited by M. Hulin (Dunod Cie, Paris, 1964), p. 677.
- ⁴⁹P. J. Stiles, E. Burstein, and D. N. Langenberg, in *Proceedings of the International Conference on the Physics of Semiconductors, Exeter, 1962*; Ref. 47, p. 557.
- ⁵⁰R. Nii, *J. Phys. Soc. Jpn.* **19**, 58 (1964).
- ⁵¹M. Numaba and Y. Uemura, *Phys. Lett.* **9**, 227 (1964); *J. Phys. Soc. Jpn.* **19**, 2140 (1964).
- ⁵²R. S. Allgaier, *J. Appl. Phys.* **32**, 2185 (1961).
- ⁵³R. S. Allgaier and B. B. Houston, *J. Appl. Phys.* **37**, 302 (1966).
- ⁵⁴Y. Sato, M. Fugimoto, and A. Kobayashi, *J. Phys. Soc. Jpn.* **19**, 24 (1964).
- ⁵⁵J. R. Dixon and M. R. Riedl, *Phys. Rev.* **38**, A873 (1965).
- ⁵⁶Y. W. Tung and Marvin L. Cohen, *Phys. Rev.* **180**, 823 (1969).
- ⁵⁷M. R. Riedl, *Phys. Rev.* **127**, 162 (1962).
- ⁵⁸W. W. Scanlon, in *Solid State Physics*, edited by F. Seitz and D. Turnbull (Academic, New York, 1959), Vol. 9, p. 83.
- ⁵⁹I. A. Drabkin, G. F. Zakharyaugina, and I. V. Nel'son, *Fiz. Tekh. Poluprovodn.* **5**, 277 (1971).
- ⁶⁰M. Escorne, A. Mauger, D. Ravot, and J. C. Achard, *J. Phys. C* **14**, 1821 (1981).
- ⁶¹A. K. Nigam and A. K. Majumdar, *Phys. Rev. B* **27**, 495 (1983).